

# Dosimetry Model for Photodynamic Therapy With Topically Administered Photosensitizers

Lars O. Svaasand, PhD, Pius Wyss, MD, Marie-Therese Wyss, MD, Yona Tadir, MD, Bruce J. Tromberg, PhD, and Michael W. Berns, PhD

Norwegian Institute of Technology, Trondheim, Norway N-7034 (L.O.S.); Beckman Laser Institute, University of California, Irvine, 92715 (L.O.S., P.W., M.-T.W., Y.T., B.J.T., M.W.B.); University of Zürich, Switzerland (P.W., M.-T.W.)

**Background and Objective:** Photodynamic therapy (PDT) based on topical application of photosensitizers has been under development over the last years. Typical applications are treatment of basal cell carcinoma of the skin and photoablation of the endometrium. The dosimetry for topically administered photosensitizers must take a time-dependent inhomogeneous drug distribution into account together with the conventional parameters such as optical scattering, absorption, and photobleaching.

**Study Design/Materials and Methods:** This study presents a dosimetry model where the cytotoxic dose is calculated in a stepwise procedure. The first step calculates the time-dependent distribution of 5-aminolevulinic acid (5-ALA) from diffusion theory. In skin this distribution is dependent on drug permeability through the stratum corneum, on the diffusivity of dermis and epidermis, on the drug clearance time, and on the conversion rate from 5-ALA to protoporphyrin IX (PpIX). In the second step the distribution of PpIX is calculated from the 5-ALA distribution found in the first step taking the dynamics of the biosynthesis of 5-ALA to PpIX and the clearance time of PpIX into account. In the third step the generation of cytotoxic singlet oxygen is calculated from the optical distribution during irradiation, taking a photobleaching mechanism into account.

**Results:** The distribution of cytotoxic oxygen is predicted from the optical dose, the drug dose, and the time between the application of the drug and the irradiation.

**Conclusion:** The presented dosimetry model is made as simple as possible, yet composite enough to enable all relevant parameters to be taken into account. The model that is based on a linear theory in a semi-infinite medium can, if required, be extended to take nonuniform and nonlinear phenomena into account.

© 1996 Wiley-Liss, Inc.

**Key words:** photodynamic therapy, dosimetry, singlet oxygen, photoproducts, 5-aminolevulinic acid, protoporphyrin IX, photobleaching, topical application, skin, endometrium

## INTRODUCTION

The rationale of the therapeutic efficacy of photodynamic therapy is based on cytotoxic products generated by excited photosensitizers [1]. The excited sensitizer can react with tissue constituents through the so-called type I process, yielding radicals or radical ions or through the

Accepted for publication October 28, 1994.

Address reprint requests to Lars O. Svaasand, Division of Physical Electronics, Norwegian Institute of Technology, Trondheim, N-7034, Norway.

Dr. Berns did not participate in the editorial review of this report.

type II process in which energy is transferred to singlet oxygen [2].

A variety of photosensitizers has demonstrated good results, e.g., hematoporphyrin derivative, chlorines, and phthalocyanins. In recent years very promising results have been obtained with the use of 5-aminolevulinic acid (5-ALA). This compound, which is a precursor in the biosynthesis of heme, stimulates the production of the photodynamically active compound protoporphyrin IX (PpIX) [3,4].

The photosensitizers can be administered either systemically or topically. Topically administered sensitizers have been used clinically in photodynamic treatment of basal cell carcinomas and experimentally in animal models for destruction of the endometrium [4,5]. The human endometrium may be ideally suited for photodynamic therapy because the thickness can be varied between 2 mm and 9 mm by manipulating the hormonal state. It should therefore be possible to optimize the thickness with respect to drug and light penetration.

The traditional dosimetry for photodynamic therapy has been developed for the case of systemic injection. In this case it is appropriate to assume a uniformly distributed drug dose in the target tissue [6,7]. The decay of the cytotoxic dose with distance from the irradiated surface is therefore only due to optical properties.

The assumption of a uniform drug distribution is certainly not valid for the case of topically applied sensitizers. The distribution of the drug with distance from the surface is then dependent on time after application, diffusion properties of the tissue, and on the vascularity. The nonuniformity in the drug distribution is an important factor in the dosimetry for photodynamic therapy of topically applied sensitizers.

The complete cytotoxic process for topically administered 5-ALA to the skin is very composite and can be divided in three stages: (1) diffusion of 5-ALA through the stratum corneum and into the epidermis and dermis, (2) metabolic synthesis of the photosensitizer (PpIX), and (3) generation of cytotoxic singlet oxygen (or possibly also radicals) by optical irradiation of PpIX. The diffusion of 5-ALA has been described for a two-layer model consisting of a diffusion barrier, i.e., the stratum corneum, on top on layers where the diffusion properties are assumed to be the same, i.e., the epidermis and dermis. The time required for the drug to diffuse to a certain depth is proportional to the square of the distance from the surface and

inversely proportional to the diffusivity. The time required for a drug to diffuse to 1 mm depth is for a diffusivity in the range of  $\kappa = 10^{-9}$ – $10^{-10}$  m<sup>2</sup>/s, ranging from 15 min to 3 h. The corresponding times required to reach 2 mm and 3 mm depths are, respectively, four times and nine times larger.

The diffusion barrier formed by the stratum corneum is characterized by a permeability. The effect of the barrier on the drug distribution is maximum immediately after application of the drug to the skin, and the relative importance of the barrier decreases with time. Thus if advantage of selective uptake of drug in regions where the stratum corneum layer is broken down, i.e., in regions of basal carcinoma, is to be taken, the irradiation should start as soon as possible. Sufficient time must, of course, be allowed for 5-ALA to diffuse to the required depth and for PpIX to be formed.

The generation of PpIX from 5-ALA is characterized by a transfer relaxation time. Correspondingly, the loss of PpIX due to decomposition and clearance from the tissue is characterized by a loss of relaxation time. The local buildup of protoporphyrin concentration will stabilize, if the local concentration of 5-ALA is constant and diffusion of PpIX can be neglected, after a time corresponding to the lost relaxation time. The situation is much more composite in the actual case where the 5-ALA concentration gradually builds up during the diffusion process. However, an order of magnitude estimate of the total buildup time for PpIX can be obtained just by adding the diffusion time to the loss relaxation time.

Optical irradiation of PpIX initiates energy transfer to the cytotoxic agent, i.e., to singlet oxygen. However, PpIX will also decompose during irradiation. The photoproducts can be photodynamically inactive, or some can be active when excited at longer wavelengths. Thus the bleaching process basically represents a loss mechanism for the active compound. The decay of the active compound can be described by a bleaching fluence parameter that corresponds the fluence required to reduce the concentration of  $1/e = 0.37$  of the initial value. The bleaching fluence of PpIX measured in vivo during treatment of human basal cell carcinoma has been reported to 17.2 J/cm<sup>2</sup>, when referred to the incident irradiation at 635 nm wavelength [16]. The residual active PpIX concentration in the upper part of the epidermis is therefore reduced to  $\sim 0.3$ – $5\%$  of the initial concentration after a typical optical dose in the range

of 50–100 J/cm<sup>2</sup>. Bleaching will therefore be a predominant phenomenon down to depths corresponding to 1–2 times the optical penetration depth, i.e., down to ~ 2–4 mm.

The limiting factor for the depth of therapeutic response for topically applied drugs is the diffusion of the sensitizer rather than the optical penetration depth. The situation is somewhat reversed compared to the case of systemically administered drugs, where the optical penetration usually is the limitation.

This report presents the framework for an appropriate dosimetry. The idea has been to develop a model that is as simple as possible, but still composite enough to allow all relevant parameters to be taken into account.

## MATERIALS AND METHODS

### Transport Mechanisms

Transport of solutes in tissues is governed by diffusion due to concentration gradients (Fick's law) and convection due pressure gradients (Darcy's law) [8,9]. The net flow of a solute can be expressed by a driving force equation of the form,

$$\vec{j} = -\kappa \text{grad}N - \gamma N \text{grad}p \quad (1)$$

where  $\vec{j}$  is flux vector and  $N$  is the concentration. The parameters  $p$  and  $\kappa$  are, respectively, the pressure and the diffusivity. The convection parameter  $\gamma$  is given by  $\gamma = Rk/\eta$ , where  $R$  is the ratio between the velocity of the solute to that of the solvent,  $k$  is the Darcy constant, and  $\eta$  is the viscosity of the solvent. The transport of a solute across vessel walls or through the interstitium of tumors is for low molecular weight hydrophilic or lipophilic solute molecules primarily determined by diffusion. For larger molecules both diffusion and convection are important [8].

The continuity equation can be expressed as

$$\text{div} \vec{j} = -\frac{\partial N}{\partial t} - \frac{N}{\tau} + q \quad (2)$$

where  $t$  is the time. The source term that characterizes the rate of generation per unit volume, is given by  $q$ . The rate of loss is assumed to be proportional to the instantaneous value of the concentration, and total loss relaxation time is  $\tau$ .

The relaxation of a photosensitizer such as , e.g., 5-aminolevulinic acid can be caused by a

range of mechanisms. Among these is decomposition due to participation in the biosynthesis of heme, i.e., generation of protoporphyrin IX and clearance due to lymphatic flow and blood perfusion. The total relaxation time can be expressed as

$$\frac{1}{\tau} = \frac{1}{\tau_{a \rightarrow p}} + \frac{1}{\tau_{cl}} \quad (3)$$

where  $\tau_{a \rightarrow p}$  and  $\tau_{cl}$  are, respectively, the relaxation time due to transfer from ALA to PpIX and the relaxation time due to all other mechanisms.

The diffusion of topically administered photosensitizers can be limited by a diffusion barrier. The stratum corneum layer that partly blocks transcutaneous transport is an example of such a barrier. The boundary condition for a diffusion barrier can be expressed as

$$j_n = K(N_0 - N_{x=0+}) = -\kappa \frac{dN}{dx} \Big|_{x=0+} \quad (4)$$

where  $j_n$  is the flux vector through the barrier. The densities  $N_0 = N_{x=0-}$  and  $N_{x=0+}$  are, respectively, the concentration outside the inside of the diffusion barrier. The barrier is located at  $x=0$  where  $x$  is the distance from the layer. The transmission through the barrier is characterized by its permeability  $K$ .

### Topical Application

The distribution in the case of a negligible convective flux, such as for drugs with small molecular weights, can be expressed from Eqs. (1) and (2) as

$$\nabla^2 N - \frac{1}{\kappa} \frac{\partial N}{\partial t} - \frac{N}{\kappa \tau} = -\frac{q}{\kappa} \quad (5)$$

where  $\gamma$  in Eq. (1) has been made equal to zero.

It now will be assumed that the drug is applied to the tissue surface at time  $t=0$ , and the concentration thereafter is kept constant. The boundary condition at  $x=0-$  is then  $N_0 = \text{const.}$  for  $t > 0$ . Furthermore, since no drug is injected, the bulk source density  $q$  is equal to zero. The equation can be solved easily by the method of Laplace transforms. The transform of Eq. (5) together

with the boundary conditions in Eq. (4), can be expressed as

$$N(s) = \frac{N_0}{s \left( 1 + \frac{\kappa}{K} \sqrt{\frac{1}{\kappa} \left( s + \frac{1}{\tau} \right)} \right)} e^{-x \sqrt{\frac{1}{\kappa} \left( s + \frac{1}{\tau} \right)}} \quad (6)$$

where  $N(s)$  is the Laplace transform of the density.

The time-dependent solution that follows from the inverse Laplace transform, can be expressed [10] as

$$N(t) = N_0 \int_0^t \left( \frac{K}{\sqrt{\kappa \pi t'}} e^{-\frac{x^2}{4\kappa t'}} - \frac{K^2}{\kappa} e^{\frac{K}{\kappa} x} e^{\frac{K^2}{\kappa} t'} \operatorname{erfc} \left( \frac{K}{\sqrt{\kappa}} \sqrt{t'} + \frac{x}{2\sqrt{\kappa t'}} \right) \right) e^{-\frac{t'}{\tau}} dt'. \quad (7)$$

The diffusivity of 5-ALA in tissue has not been reported. However, an order of magnitude estimate can be obtained by using the diffusivities for compounds with approximately the same molecular weight. The molecular weight of 5-ALA is 168 and typical values for the diffusivity of glucose (mol.wt. 180) at 37°C are  $0.69 \cdot 10^{-10}$  m<sup>2</sup>/s (brain),  $1.7 \cdot 10^{-10}$  m<sup>2</sup>/s (human aorta-intima) and  $0.88 \cdot 10^{-9}$  m<sup>2</sup>/s (plasma) [9]. The corresponding values for oxygen, acetic acid (mol.wt. 60), and sucrose (mol.wt. 342) in water at 20°C are, respectively,  $1.8 \cdot 10^{-9}$ ,  $0.88 \cdot 10^{-9}$ , and  $0.45 \cdot 10^{-9}$  m<sup>2</sup>/s. [11]

The values for permeability of 5-ALA in the stratum corneum layer of intact skin and of skin overlying basal cell carcinomas are equally not reported. However, the ratio between the PpIX fluorescence in regions with basal cell carcinoma and normal adjacent skin has been found to be  $\sim 10$ – $15$ . If it is hypothesized that this ratio corresponds to the concentration ratio of ALA in the layer just below the diffusion barrier and that the barrier is strongly reduced in the tumorous region, it is possible to make an estimate of the permeability. A concentration ratio of  $10$ – $15$  obtained 2–4 h after topical application on a tissue with diffusivity in the range of  $\kappa = 10^{-9}$ – $10^{-10}$  m<sup>2</sup>/s corresponds, according to Eq. (7), to a permeability of an intact stratum corneum in the range of  $K = 10^{-7}$ – $10^{-8}$  m/s. The lower limit for the corresponding permeability in the tumorous region is then about  $K = 10^{-6}$  m/s (see also Fig. 6). The values can, however, be significantly higher if

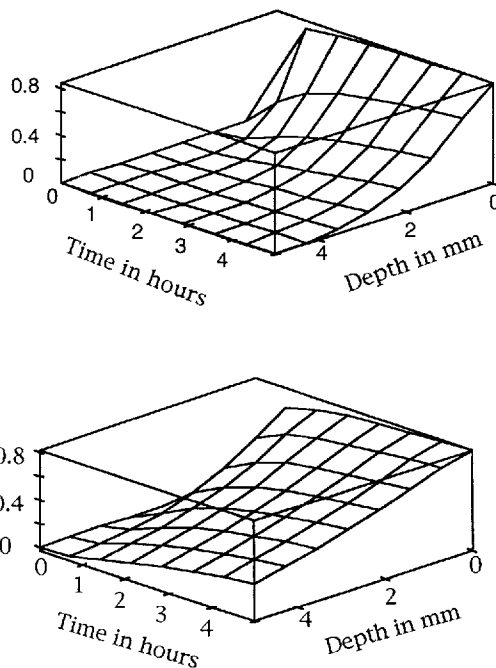


Fig. 1. Density profile vs. time (in hr) and depth (in mm). Maximum value is normalized to unity, i.e.,  $N_0 = 1$  m<sup>-3</sup>.  $K = 10^{-6}$  m/s,  $\tau = 24$  h. (a) (upper graph):  $\kappa = 10^{-10}$  m<sup>2</sup>/s; (b) (lower graph):  $\kappa = 10^{-9}$  m<sup>2</sup>/s.

permeability enhancing compounds such as DMSO and Azone are used.

Examples of predicted spatial and temporal dependence of density profiles are shown in Figure 1. The calculations that are based on Eq. (7) are shown for two different diffusivities,  $\kappa = 10^{-9}$  m<sup>2</sup>/s and  $\kappa = 10^{-10}$  m<sup>2</sup>/s. The relaxation time is  $\tau = 24$  h, and the permeability corresponds to the value estimated for tumorous regions, i.e.,  $K = 10^{-6}$  m/s. The graphs demonstrate that the barrier blocks the diffusion efficiently for a period up to 1 h. The effect of the barrier is, however, insignificant after 2 h, and the concentration at the inside of the barrier is then more than 80% of the outside value. After a 4-h period,  $\sim 50\%$  of the value is reached at a depth of 1 mm for  $\kappa = 10^{-10}$  m<sup>2</sup>/s, whereas the corresponding depth for  $\kappa = 10^{-9}$  m<sup>2</sup>/s is in the range of 2.5 mm.

In the time region where  $t \ll \tau$ , the expression for the density of ALA as given in Eq. (7) can be approximated to

$$N(t) = N_0 \left( \operatorname{erfc} \left( \frac{x}{2\sqrt{\kappa t}} \right) - \frac{K}{\kappa} e^{\frac{K}{\kappa} x} \operatorname{erfc} \left( \frac{K}{\sqrt{\kappa}} \sqrt{t} + \frac{x}{2\sqrt{\kappa t}} \right) \right). \quad (8)$$

If, however, the time scale is much larger than the diffusion time, i.e.,  $t \gg x^2/\kappa$ , the distribution can be approximated by the steady-state solution:

$$N(t \rightarrow \infty) = \frac{N_0}{1 + \frac{1}{K} \sqrt{\frac{\kappa}{\tau}}} e^{-\frac{x}{\sqrt{\kappa t}}}. \quad (9)$$

The factor  $(1 + 1/K\sqrt{\kappa/\tau})^{-1}$  represents the steady-state depletion of the drug concentration across the diffusion barrier. The barrier is only significant for permeabilities in the range where  $K \ll \sqrt{\kappa/\tau}$ . For example, in the case of a diffusivity of  $\kappa = 10^{-9} \text{ m}^2/\text{s}$  together with a relaxation time of  $\tau = 24 \text{ h}$ , this condition corresponds to a permeability much less than  $K = 10^{-7} \text{ m/s}$ . The exponential factor in Eq. (9) represents the steady-state decay with distance from the surface. The penetration depth of the drug, i.e., the distance corresponding to a decay of the concentration by a factor of  $1/e = 0.37$ , is given by the parameter  $\delta_d$ ,

$$\delta_d = \sqrt{\kappa\tau}. \quad (10)$$

High values for the penetration depth are found in tissues with high diffusivity and low clearance rate, e.g., the values  $\kappa = 10^{-9} \text{ m}^2/\text{s}$  and  $\tau = 24 \text{ h}$  give a penetration depth of  $\delta_d = 9 \text{ mm}$ . Correspondingly low values are found in tissues with low diffusivity and high clearance rate, e.g., the penetration depth in the case of  $\kappa = 10^{-10} \text{ m}^2/\text{s}$  and  $\tau = 4 \text{ h}$  is only  $\delta_d = 1.2 \text{ mm}$ .

### Generation of Protoporphyrin IX

The equation of continuity for protoporphyrin can be expressed as

$$\text{div} \vec{j}_p = -\frac{\partial P}{\partial t} - \frac{P}{\tau_p} + q_p \quad (11)$$

where  $P$  is the local concentration of PpIX,  $\vec{j}_p$  is the corresponding flux vector,  $\tau_p$  is the protoporphyrin relaxation time, and  $q_p$  is the source density. In the case of negligible diffusion and convection this equation can be expressed as

$$0 = -\frac{dP}{dt} - \frac{P}{\tau_p} + \epsilon_p \frac{N}{\tau_{a \rightarrow p}} \quad (12)$$

where source term has been expressed by

$$q_p = \epsilon_p \frac{N}{\tau_{a \rightarrow p}}.$$

The parameter  $\epsilon_p$  characterizes the yield of this process.

The Laplace transform  $P(s)$  of the time-dependent protoporphyrin concentration follows from Eq. (12):

$$P(s) = \frac{\epsilon_p}{\tau_{a \rightarrow p}} \frac{1}{s + \frac{1}{\tau_p}} N(s) \quad (13)$$

where  $N(s)$  is the Laplace transform of the ALA concentration given in Eq. (6). The time-dependent concentration can be expressed by a convolution integral of the form [10] as

$$P(t) = \frac{\epsilon_p}{\tau_{a \rightarrow p}} e^{-\frac{t}{\tau_p}} * N(t) = \frac{\epsilon_p}{\tau_{a \rightarrow p}} \int_0^t e^{-\frac{t-t'}{\tau_p}} N(t') dt'. \quad (14)$$

In regions with a strongly reduced diffusion barrier such as in a basal cell carcinoma where the stratum corneum is broken down, the 5-ALA concentration in the upper part of the epidermis can be taken to be constant and equal to  $N_0$ . In such a case, Eq. (14) can be simplified to

$$P(t) = \frac{\epsilon_p}{\tau_{a \rightarrow p}} e^{-\frac{t}{\tau_p}} * N_0 = \frac{\epsilon_p \tau_p}{\tau_{a \rightarrow p}} \left(1 - e^{-\frac{t}{\tau_p}}\right) N_0. \quad (15)$$

When the protoporphyrin relaxation time is large compared to the relevant time scale, i.e., to the diffusion time  $t$  ( $\tau_p \gg t$ ) Eq. (14) reduces to

$$P(t) = \frac{\epsilon_p}{\tau_{a \rightarrow p}} \int_0^t N(t') dt'. \quad (16a)$$

If, however, the relaxation mechanism of PpIX is fast compared to the diffusion time for ALA, i.e.,  $\tau_p \ll t$  the equation reduces to

$$P(t) = \epsilon_p \frac{\tau_p}{\tau_{a \rightarrow p}} N(t). \quad (16b)$$

The protoporphyrin concentration is thus proportional to the time integral of the ALA concentration when the relaxation of PpIX is slow compared to the diffusion time  $t$ , whereas it is proportional to the instantaneous value of the ALA concentration in the case of fast relaxation.

## Selectivity

The selectivity of the photodynamic response to normal and malignant tissues may be dependent of a variety of parameter such as different conversion efficiency of ALA to PpIX, different localization of PpIX with the cell, and different diffusion/clearance properties. A major mechanism for the increased photosensitizer concentration in the region of the skin with basal cell carcinoma is, as discussed earlier, believed to be the breakdown of the stratum corneum. The present discussion is therefore limited to this particular mechanism. The impact of a diffusion barrier on the sensitizer concentration is maximal immediately after the topical application, and the influence decreases with time until the steady-state value is reached. The maximum ratio between the sensitizer concentration in the tumorous region and in the normal skin is given by the ratio between the permeabilities (see Eq.7). The corresponding steady-state ratio follows from Eq. (9). The upper and lower limits of the time-dependent ratio can thus be expressed as

$$\frac{K_t}{K_n} > \frac{N_t}{N_n} > \frac{1 + \frac{1}{K_n} \sqrt{\frac{\kappa}{\tau}}}{1 + \frac{1}{K_t} \sqrt{\frac{\kappa}{\tau}}} \quad (17)$$

where  $N_t$  and  $K_t$  are, respectively, the drug concentration and the epidermal permeability in the tumorous region. The corresponding parameters in normal skin are  $N_n$  and  $K_n$ . The diffusivity and relaxation time are both assumed to be the same in the two regions.

The steady-state ratio is, under these conditions, independent on depth. The ratio approaches unity if the permeabilities are much larger than the quantity  $\sqrt{\frac{\kappa}{\tau}}$ , whereas it approaches  $\frac{K_t}{K_n}$  for small permeabilities.

Figure 2 shows an example of the concentration ratio between regions where the permeabilities differs by a factor of 10. The figure shows the ratio versus time and distance from the surface (Eq.7). The diffusivity is assumed to be the same, and the relaxation time is taken to be infinitely long. A maximum ratio of 10 is obtained immediately after the topical application, and the ratio decreases monotonously with time to the steady-state value of 1 as follows from Eq. (17). The

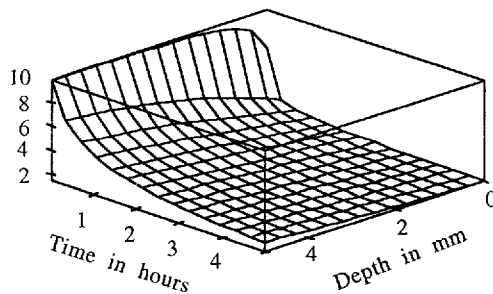


Fig. 2. Ratio of photosensitizer concentration. The time scale is from 30 s to 5 h after topical application of ALA.  $K_t = 10^{-6}$  m/s,  $K_n = 10^{-7}$  m/s,  $\kappa = 10^{-10}$  m<sup>2</sup>/s,  $\tau = \infty$ .

graph that covers the time scale from 0.5 min to 5 h also demonstrates the very rapid decrease in the ratio close to the surface.

The fact that the maximum concentration ratio is obtained immediately after application does not, however, mean that the optimum time for treatment is shortly after application. It is, of course, necessary to wait until an adequate quantity of the drug has diffused to the relevant depth. The order of magnitude of this time delay,  $\Delta t$ , is provided so that the distance  $x$  is smaller than the penetration depth  $\sqrt{\kappa\tau}$ , given by the diffusion time for a lossless medium, [12]

$$\Delta t \approx \frac{x^2}{\kappa} \quad (18)$$

Typical delays in the case of 1-mm and 2-mm-thick lesions are, respectively,  $\sim 3$  h and 12 h for a diffusivity of  $\kappa = 10^{-10}$  m<sup>2</sup>/s. The corresponding delays in the case of a diffusivity of  $\kappa = 10^{-9}$  m<sup>2</sup>/s are  $\sim 15$  min and 1 h for, respectively, 1 and 2 mm thicknesses.

The time required to establish the drug concentration at depths larger than the penetration depth is approximately [12]

$$\Delta t \approx \frac{x}{\sqrt{\frac{\kappa}{\tau}}} \quad (19)$$

The transit time  $\Delta t$  over a distance corresponding to the penetration depth, i.e.,  $x = \sqrt{\kappa\tau}$  is thus approximately equal to the relaxation time  $\tau$ . Correspondingly, the transit time for a distance equal to  $n$  times the penetration depth is equal to  $n$  times the relaxation time. The concentration will

be, as discussed previously, significantly depleted for depths larger than the penetration depth. The penetration depth of the drug might therefore represent an upper limit for the thickness of lesions that can be treated.

### Optical Distribution

The optical distribution in dermis is very complex. The optical properties such as absorption and scattering coefficients are quite different in the various skin layers. A detailed analysis of the light distribution in the epidermis and in the upper part of the dermis requires an optical model that takes the multilayered structure into account [17]. However, the cytotoxic dose delivered to regions close to the site of irradiation will be limited by the photo-bleaching of the drug rather than by the optical dose. The present discussion therefore uses a simplified optical model where the light distribution is approximated by a single exponential term [7,13,14]. This model, which has very limited validity in the epidermis/papillary dermis region, has proved to be quite good at depths larger than  $\sim 1$  mm from the irradiated surface. The optical fluence rate can then be expressed as

$$\varphi = k_p I e^{-\frac{x}{\delta}} \quad (20)$$

where  $\varphi$  is the in situ optical fluence rate and  $I$  is the incident irradiation. The optical penetration depth, i.e., the distance corresponding to a decay in the fluence rate by a factor  $1/e = 0.37$ , is given by  $\delta$ . The parameter  $k_p$ , which is dependent on the optical boundary conditions at the air/tissue interface and on the detailed optical structure of the upper dermal layers, serves as a dimensionless coupling coefficient relating the fluence rate to the incident irradiation. The total in situ optical dose, i.e., the fluence delivered locally during the irradiation, can be expressed as

$$\psi = \int_0^t \varphi dt' = k_p e^{-\frac{x}{\delta}} \int_0^t I dt' = k_p \psi_{inc} e^{-\frac{x}{\delta}} \quad (21)$$

where  $\psi_{inc}$  is the incident optical fluence. The fluence in the surface layer of the tissue is because of backscattering and total internal reflection at the surface, usually a factor 2–3 times larger than the incident optical fluence. Typical values for the optical penetration depth in the wavelength region from 600–800 nm are in the range of  $\delta = 2-4$  mm

for most tissues. The penetration depths in melanotic melanomas are, however, only about one-tenth of the values, i.e., in the range of  $\delta = 0.3-0.5$  mm.[14]

### Photosensitizer Bleaching and Generation of Photoproducts

Photobleaching of a sensitizer depletes the photodynamically active compounds simultaneously with the formation of new photoproducts. Provided that clearance and diffusion are negligible during irradiation, this process can be expressed by

$$\begin{aligned} \frac{dP}{d\psi} &= \frac{P}{\theta} = -\frac{P}{\theta_1} - \frac{P}{\theta_2} \\ \frac{d\Pi}{d\psi} &= -\frac{\Pi}{\theta_3} + \epsilon_{pp} \frac{P}{\theta_2} \end{aligned} \quad (22)$$

where  $\psi$  is the optical fluence (or dose). The concentrations  $P$  and  $\Pi$  are, respectively, the concentration of PpIX and of one of the generated photoproducts. The yield of the conversion process from protoporphyrin to the photoproduct is characterized by  $\epsilon_{pp}$ . The bleaching fluence that corresponds to a reduction of PpIX to  $1/e = 0.37$  of its initial concentration is given by  $\theta$ . This parameter can be subdivided into a parameter  $\theta_2$  characterizing transfer to one particular photoproduct, together with a parameter  $\theta_1$  characterizing all other photo-induced loss processes. The parameter  $\theta_3$  characterizes the total relaxation fluence of the photoproduct. The solution of Eq. (22) can be expressed as

$$\begin{aligned} P &= P_0 e^{-\frac{\psi}{\theta}} \\ \Pi &= \frac{\epsilon_{pp} P_0}{\theta_2 \left( \frac{1}{\theta_3} - \frac{1}{\theta} \right)} \left( e^{-\frac{\psi}{\theta}} - e^{-\frac{\psi}{\theta_3}} \right) \end{aligned} \quad (23)$$

where  $P_0$  is the in situ concentration of PpIX before optical irradiation (see Eq. 14).

The available data on the photo-decomposition parameters are very limited. However, the bleaching fluence of hematoporphyrin derivative has been reported as  $\theta = 75 \text{ J/cm}^2$  at 630 nm wavelength [7], and in vivo measurements on bleaching of PpIX during treatment of human basal cell carcinoma have been reported to be 17.2

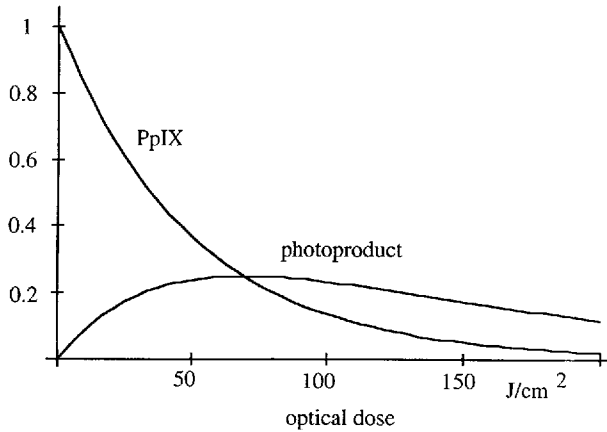


Fig. 3. Normalized concentration of protoporphyrin IX and of a photoproducts versus optical dose in  $\text{J}/\text{cm}^2$ . Parameters  $\theta_1 = \theta_2 = 100 \text{ J}/\text{cm}^2$  and  $\theta_3 = 100 \text{ J}/\text{cm}^2$ .

$\text{J}/\text{cm}^2$ , when referred to the incident irradiation. The treatment was done with a copper vapor pumped dye laser at 635 nm wavelength, and the bleaching was determined from measuring fluorescence excited with 405 nm radiation. This bleaching value will, when corrected for the 2–3 times higher epidermal fluence rate than the incident irradiation, correspond to a bleaching fluence in the range  $\theta = 35\text{--}50 \text{ J}/\text{cm}^2$  [16].

An example of the depletion of the initial sensitizer together with generation of a photoproduct, is shown in Fig. 3. The fluence parameters  $\theta_1$  and  $\theta_2$  are both taken equal to  $100 \text{ J}/\text{cm}^2$  and  $\theta_3 = 100 \text{ J}/\text{cm}^2$ . The sensitizer concentration decreases exponentially in accordance to a total bleaching fluence of  $\theta = 50 \text{ J}/\text{cm}^2$ , whereas the photoproducts reaches a maximal value at a fluence of  $\psi = \frac{\theta\theta_3}{\theta_3 - \theta} \ln \frac{\theta_3}{\theta}$ , i.e.,  $\psi = 69 \text{ J}/\text{cm}^2$ .

This analysis describes how the creation and destruction of a particular photoproduct can be followed. It should be pointed out, however, that the creation of a photoproduct does not imply that it will be absorbed at the same wavelength as the excitation light, nor that it will be necessarily photodynamically active. However, the contribution to the singlet oxygen production from the photoproducts that generally have absorption peaks at longer wavelengths might be important when broad-banded light sources are used during therapy.

## RESULTS

The question of continuity for singlet oxygen can be expressed as

$$\text{div} \vec{j}_s = -\frac{\partial S}{\partial t} - \frac{S}{\tau_s} + q_s \quad (24)$$

where  $S$  is the local concentration of singlet oxygen,  $j_s$  is the flux vector,  $\tau_s$  is the total singlet oxygen relaxation time, and  $q_s$  is the source density.

The generation rate of singlet oxygen is proportional to the sensitizer concentration and to the optical fluence. The source term can therefore be expressed as  $q_s = \epsilon_s P \phi$ , where  $\epsilon_s$  characterizes the efficiency of the porphyrin to singlet oxygen process. The lifetime of singlet oxygen in tissue is in the order of microseconds [15]. The generation of singlet oxygen and the cytotoxic reaction will therefore take place within the same cell, or at least in the immediate proximity of that cell. The diffusion of singlet oxygen is therefore of no importance and the flux vector can be neglected [7]. The term containing the time derivative can further on also be neglected since the relaxation of singlet oxygen is very fast compared to the irradiation time during PDT. The singlet oxygen concentration can therefore be expressed (Eq. 24) as

$$S = \tau_s \epsilon_s P \phi. \quad (25)$$

The amount of singlet oxygen generated during an interval of time,  $dt$ , during irradiation is given by  $q_s$ . The total amount of singlet oxygen,  $\Sigma$ , being generated during the entire irradiation period can then be expressed as

$$\Sigma = \int_t^{t+\Delta t_r} q_s dt = \int_t^{t+\Delta t_r} \epsilon_s P \phi dt = \epsilon_s \theta \left(1 - e^{-\frac{\psi}{\theta}}\right) P_0 \quad (26)$$

where  $t$  is the time between the application of the drug and the onset of the irradiation, and  $\Delta t_r$  is the duration of the irradiation. In the integration of Eq. (26), it is assumed that no diffusion or clearance of PpIX takes place during irradiation. The only depletion mechanism for protoporphyrin during the delivery of the optical dose  $\psi$  is therefore photobleaching (Eq. 23). The concentration before irradiation,  $P_0$ , is given by Eq. (14) when  $t$  in that equation is interpreted as the interval of time between the application of the drug and the irradiation.

The cytotoxic dose experienced locally by the tissue will be proportional to the total amount of singlet oxygen generated in that region. The in

situ cytotoxic dose,  $D(x)$ , can therefore be expressed, Eqs. (7), (14), and (26) as

$$D(x) = \alpha \Sigma = \alpha N_0 \theta \frac{\epsilon_s \epsilon_p}{\tau_{l \rightarrow p}} \left( 1 - e^{-\frac{\psi}{\theta}} \right) \cdot \int_0^t e^{-\frac{t-t'}{\tau_p}} \left( \int_0^{t'=t''} \left( \frac{K}{\sqrt{\kappa \pi t'}} e^{-\frac{x^2}{4\kappa t'}} - \frac{K^2}{\kappa} e^{\frac{K}{\kappa} x} e^{-\frac{K^2}{\kappa} t'} \right) \operatorname{erfc} \left( \frac{K}{\sqrt{\kappa}} \sqrt{t'} + \frac{x}{2\sqrt{\kappa t'}} \right) e^{-\frac{t'}{\tau} dt'} \right) dt'' \quad (27)$$

where  $\alpha$  is a normalization constant. This parameter can be chosen in such a manner that a dose equal to unity, i.e.,  $D=1$ , corresponds to 50% probability for local tissue necrosis.

The distribution of the cytotoxic dose in tissue is visualized in Figure 4. The maximum value of the cytotoxic dose, i.e., the amount of singlet oxygen that will be generated after applying an infinite large optical dose to regions with maximal photosensitizer concentration, is, in Figures 4–6, normalized to unity. The relaxation time of 5-ALA is further on assumed to be much larger than the time  $t$  (see also Eq. 8), and the PpIX concentration is taken to be proportional to the ALA concentration (see also Eq. 16). The value of  $\kappa = 10^{-9} \text{ m}^2/\text{s}$  that corresponds to the diffusion constant for glucose in serum is selected for the diffusivity. The value for the permeability, i.e.,  $K = 10^{-6} \text{ m/s}$ , corresponds to regions with an insignificant diffusion barrier. This value is presumably representative for regions of the skin where the diffusion barrier is broken down by basal cell carcinomas. The distribution is shown versus distance from the surface and versus irradiant optical dose. Figure 4a gives the distribution in the case of a 2-hr period between the topical application and the irradiation, and Figure 4b gives the corresponding values for a 4-h period.

The corresponding results for a high diffusion barrier such as in the case of an intact stratum corneum are shown in Figure 5. Figure 5a gives the distribution in the case of  $K = 10^{-7} \text{ m/s}$  and Figure 5b gives the results for  $K = 10^{-8} \text{ m/s}$ . The presence of a diffusion barrier significantly reduces the cytotoxic dose: the dose in Figure 5b is about a factor of about 20 less than the dose given in Figure 4b.

The distribution shown in Figure 6 is calculated for the same parameters as given in Figure 4b with the exception of the diffusivity, which has been reduced from the serum value to a value

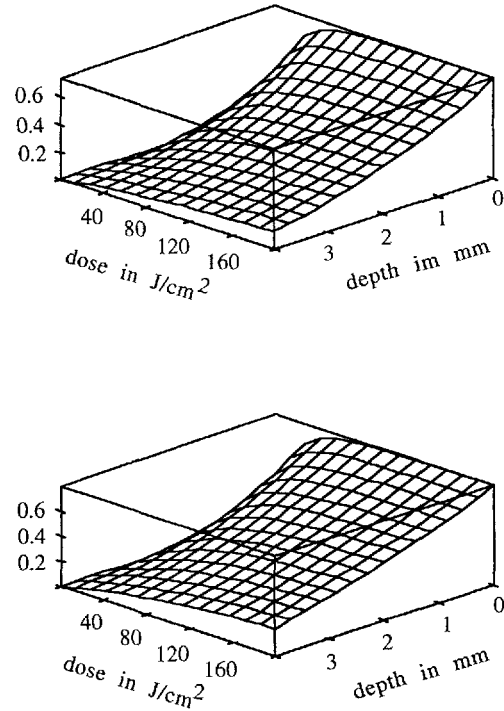


Fig. 4. Distribution of normalized cytotoxic dose.  $K = 10^{-6} \text{ m/s}$ ,  $\kappa = 10^{-9} \text{ m}^2/\text{s}$ ,  $\theta = 50 \text{ J/cm}^2$ ,  $\delta = 2 \text{ mm}$ ,  $k_p = 3$ . (a) (upper graph):  $t = 2 \text{ h}$ ; (b) (lower graph):  $t = 4 \text{ h}$ .

characteristic for brain and human aorta-intima, i.e.,  $\kappa = 10^{-10} \text{ m}^2/\text{s}$  [8]. The reduced diffusivity slightly enhances the dose close to the surface. However, it causes a much stronger fall off with distance. The dose shown in Figure 6 is reduced to approximately the half at a depth of 1 mm, whereas the corresponding distance is  $\sim 3 \text{ mm}$  for the case shown in Figure 4b.

## CONCLUSION

The discussed dosimetry model with a single diffusion barrier on a semi-infinite medium is, of course, a very simplified approach to the actual clinical situation. However, even a simple model can be very useful for improving the dosimetry. For example, by monitoring the time dependence of the drug concentration in the surface layer by fluorescence, it should be possible to evaluate the permeability of the stratum corneum together with the diffusivity of the underlying tissue. These values can then be used to predict the distribution in deeper layers.

The model can, however, be extended easily to the more complex multilayer case. Such an extension might be necessary in the case of endo-

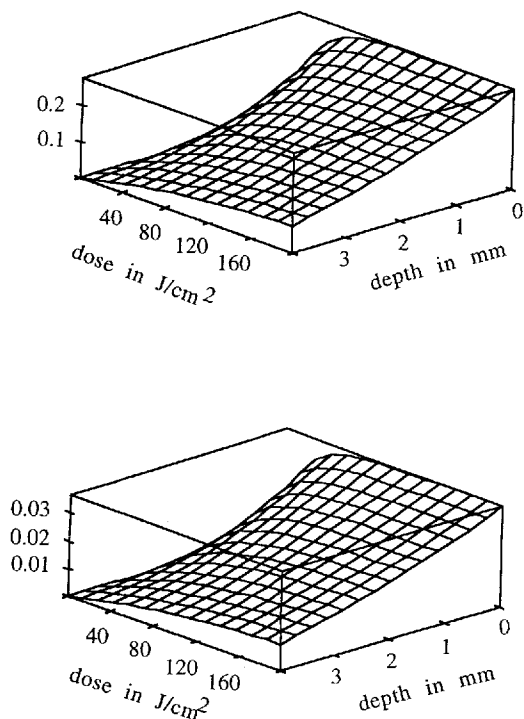


Fig. 5. Distribution of normalized cytotoxic dose.  $t = 4$  h.,  $\kappa = 10^{-9}$  m<sup>2</sup>/s,  $\theta = 50$  J/cm<sup>2</sup>,  $\delta = 2$  mm,  $k_p = 3$ . (a) (upper graph):  $K = 10^{-7}$  m/s; (b) (lower graph)  $K = 10^{-8}$  m/s.

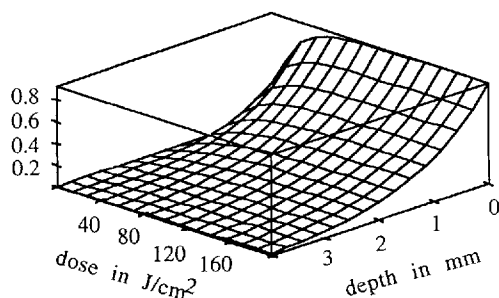


Fig. 6. Distribution of normalized cytotoxic dose.  $K = 10^{-6}$  m/s,  $\kappa = 10^{-10}$  m<sup>2</sup>/s,  $\theta = 50$  J/cm<sup>2</sup>,  $\delta = 2$  mm,  $k_p = 3$ ,  $t = 4$  h.

metrial ablation since the diffusion properties as well as the protoporphyrin generation efficiency might differ in the endometrium and in the myometrium.

The simplified optical model, which gives an adequate description of the optical distribution in the deeper layer, might be equally extended to a more precise model [17]. This extension is necessary in particular in the case of high drug concentration and low light doses. In such a case bleaching might be unimportant and the more precision will be required in the determination of the optical dose.

In conclusion, the presented simplified dosimetry model might be useful in understanding the relevance of the different mechanisms. Further on it should also serve to draw attention to the various parameters that have to be determined before a reliable dosimetry model is available in the clinic.

## ACKNOWLEDGMENTS

This work was supported by grants: NIH # 2R01 CA32248 and #5P41 RR01192, DOE #DE-FG03-91ER61227 and ONR # N00014-91-C-0134, Academ. Nachwuchsfoerderung, University of Zürich, Switzerland.

## REFERENCES

1. Dougherty TJ. Photodynamic therapy (PDT) of malignant tumors. *CRC Crit Rev Oncol/Hematol* 1984; 2(2): 83–116.
2. Foote CS. Chemical mechanism of photodynamic action. In: CJ Gomer, ed. *Advanced Optical Technologies*. SPIE Inst. Ser. 1990; IS6:115–129.
3. Yang JZ, van Vugt DA, Kennedy JC, Reid RL. Evidence of lasting functional destruction of the rat endometrium after 5-aminolevulinic acid-induced photodynamic ablation: Prevention of implantation. *Am J Obstet Gynecol* 1993; 168(3):995–1001.
4. Kennedy JC, Pottier RH, Pross DC. Photodynamic therapy with endogenous porphyrin IX: Basic principles and present clinical results. *J Photochem Photobiol* 1990, B 6, pp 143–148.
5. Wyss P, Tromberg BJ, Wyss MTh, Krasieva T, Schell M, Berns MW, Tadir Y. Photodynamic destruction of endometrial tissue using 5-aminolevulinic acid (5-ALA) in rats and rabbits. *Am J Obstet Gynecol* 1994; 171(5): 1176–1183.
6. Grossweiner LI. Light dosimetry for photodynamic therapy treatment planning, *Lasers Surg Med* 1991; 11:165–173.
7. Svaasand LO, Potter W. The Implications of Photobleaching for Photodynamic Therapy. In: "Photodynamic Therapy: Basic Principles and Clinical Aspects." Henderson B, and Dougherty T.J., eds. New York: Marcel Dekker, 1992, pp 369–384.
8. Jain RK. Transport of molecules across tumor vasculature, *Cancer Metastasis Rev* 1987; 6:559–593.
9. Jain RK. Transport of molecules in the tumor interstitium: A review. *Cancer Res* 1987; 47:3039–3051.
10. Abramowitz M, Stegun IA. "Handbook of Mathematical Functions." Washington, DC: National Bureau of Standards, Appl. Math. Ser. 55, 1964.
11. "CRC Handbook of Appl. Eng. Science." 1970.
12. Svaasand LO, Tromberg BJ, Haskell RC, Tsay TT, Berns MW. Tissue characterization and imaging using photon density waves, *Optical Eng* 1993; 32(2):258–266.
13. Profio AE, Doiron DR. Transport of light in tissue in photodynamic therapy. *Photochem Photobiol* 1987; 46(5), 591–599.
14. Svaasand LO, Morinelli E, Gomer CJ. Laser-induced hyperthermia in the treatment of ocular tumors: Experi-

- mental evaluation of temperature rise in rabbit's eye. SPIE 1989; 1321:77–96.
5. Moan J. On the diffusion length of singlet oxygen. *Photochem Photobiol* 1990; 6:343–344.
  6. Hoeydalsvik E. Characterization of the Distribution of Porphyrins in Malignant Tumors by Fluorescence. M.Sc. thesis, Division of Physical Electronics, Norwegian Institute of Technology, 1994.
  17. Keijzer M, Star WM, Storchi PRM. Optical diffusion in layered media. *Appl Optics* 1988; 27:1820–1824.